Physica D 31 (1988) 117–126
North-Holland, Amsterdam

FOURIER ANALYSIS OF MULTI-FREQUENCY DYNAMICAL SYSTEMS

Seunghwan KIM*, Stellan OSTLUND and Gang YU
Department of Physics, University of Pennsylvania, Philadelphia, PA 19104, USA

Received 13 February 1987
Revised manuscript received 4 November 1987
Communicated by R.M. Westervelt

The Fourier spectrum of a multiply periodic system appears complex due to resonances at integer combinations of the fundamental frequencies. We show how to "reorder" the peaks in the Fourier spectrum to yield a simpler structure which reveals important aspects of the time series which are not clearly seen in the ordinary Fourier transform. As examples, we study time series from circle and torus maps, and from experimental data by Gollub and Benson.

1. Introduction

Dynamical systems with several fundamental frequencies have been the subject of active research [1–5]. In these systems, the competition of several frequencies results in many interesting phenomena, including the quasiperiodicity, mode-locking, and chaos. One of the most important methods for probing multi-frequency systems has been spectral analysis [5–7] particularly in the analysis of experimental data. The Fourier analysis yields information about the number and values of fundamental frequencies as well as information about the relative importance of various harmonics.

However, as it is often displayed, the Fourier spectrum yields little other information. The spectrum is dominated by a few major peaks corresponding to the fundamental frequencies, but it is not easy to understand the organization of the strengths of the higher harmonics. In this paper, we show how to "reorder" the Fourier spectra to view the organization of the spectrum by extending the analysis of the two-frequency spectrum as discussed in ref. [2] to three or more frequencies.

*Present address: Mathematical Science Institute, White Hall, Cornell University, Ithaca, NY 14853, USA.

The organization of the paper is as follows. In section 2, we briefly review the ordinary Fourier spectral analysis of quasiperiodic time series and the reordering scheme discussed in ref. [2]. We also discuss the relevance of the reordered spectrum to the study of the chaos transition. In section 3, examples of time series from maps and a hydrodynamic experiment of Gollub and Benson [6] are analyzed according to our scheme. In section 4, we end by discussing several possible complications when our analysis is applied to experimental data.

2. Reordering scheme

2.1. *Overview of the ordinary Fourier analysis*

Assume that two fundamental frequencies ω_1 and ω_2 determine the dynamics of a physical system, and that $x(t)$ is a dynamical variable as a function of time t. The existence of two independent frequencies implies that we can write

$$x(t) = \sum_{n,n'} a(n,n')\, e^{i(n\omega_1 + n'\omega_2)t}, \tag{2.1}$$

where the summation is over all pairs of integers. In a convection experiment, $x(t)$ could be, for example, a local velocity or temperature of the fluid. We obtain a discrete time series, $x_l =$

$x(2\pi l/\omega_2)$, by "strobing" the physical system at time intervals corresponding to one of the fundamental frequencies, say ω_2. From eq. (2.1) we see that

$$x_l = \sum_{n=-\infty}^{\infty} A_n e^{2\pi i l n \rho}, \tag{2.2}$$

where $\rho = \omega_1/\omega_2$ and

$$A_n = \sum_{n'=-\infty}^{\infty} a(n, n'). \tag{2.3}$$

We can define the function

$$g(x) = \sum_{n=-\infty}^{\infty} A_n e^{2\pi i x n}. \tag{2.4}$$

We say that $g(x)$ *generates* x_l since $x_l = g(l\rho)$. Provided that $x(t)$ is sufficiently smooth, $g(x)$ will be analytic.

We define the spectral amplitude $s(\omega)$ of x_l to be

$$s(\omega) = \lim_{N\to\infty} \frac{1}{N} \sum_{l=0}^{N-1} x_l e^{-2\pi i l \omega}. \tag{2.5}$$

Let $\rho_n \equiv \{p_n/q_n\}_{n=0}^{\infty}$ be a set of rational approximants to ρ such that $\lim_{n\to\infty}(p_n/q_n) = \rho$ with $|p_n/q_n - \rho| > |p_{n+1}/q_{n+1} - \rho|$ and $q_n < q_{n+1}$. We also choose $\{p_n/q_n\}$ to be optimal, in the sense that $|q_n\rho - p_n| < |r\rho - p|$ for any $r < q_n$. Although the number ρ can be rational, we are more interested in the case where it is irrational. For a given finite time series, we can best approximate the Fourier spectrum $s(\omega)$ by choosing the number of data points used to compute the Fourier transform to be q_n. We shall denote the resultant approximation to $s(\omega)$ by s_n, which is defined by

$$s_n(m) = \frac{1}{q_n} \sum_{l=0}^{q_n-1} x_l e^{-2\pi i l m/q_n}. \tag{2.6}$$

We then have

$$s(\omega) = \lim_{n\to\infty} s_n([\omega q_n]), \tag{2.7}$$

where $[x]$ indicates the closest integer to x.

The previous discussion focused on the spectral quantities related to time series taken from a continuously evolving system. In numerical experiments, it is easier to work with a mapping "f" which generates the discrete time series x_l explicitly. The "standard" circle map f is defined by

$$f_{a,\Omega}(x) = x + \Omega - \frac{a}{2\pi}\sin(2\pi x), \tag{2.8}$$

where a and Ω are fixed parameters. The winding number ρ is defined as the average "rotation" rate of the mapping

$$\rho = \rho(a, \Omega) = \lim_{n\to\infty} \frac{f^n_{a,\Omega}(x_0) - x_0}{n}, \tag{2.9}$$

where f^n indicates repeated compositions of f with itself. The physical interpretation of ρ corresponds to that defined for the continuously evolving system. The variable x_l is then taken to be

$$x_l = f^l(x_0) - l\rho - x_0. \tag{2.10}$$

It is known that the function g which generates x_l is C_∞ if both f and its inverse are C_∞ [1, 2, 8].

A typical quasiperiodic spectrum for a standard circle map with $\rho = \sigma_G = (\sqrt{5} - 1)/2$ and $a = 0.98$ is shown in fig. 1. We have made a log plot of m vs $|s_{17}(m)|^2$ using the rational approximant, $\rho_{17} \equiv p_{17}/q_{17} = 2584/4181$. This particular choice of the rational approximant is from the Farey tree algorithm [9, 10]. Note that only left half of the spectrum is shown. The spectrum for $\frac{1}{2} < \omega < 1$ can be obtained by the mirror reflection about $\omega = \frac{1}{2}$. A major peak is seen at $\omega = 1 - \rho_{17} = 1597/4181$. A mirror image peak is located at $\omega = \rho_{17} = 2584/4181$. Another peak is seen at $\omega = \langle 2\rho_{17}\rangle_1 = 987/4181$ where $\langle x\rangle_y$ indicates x modulo y. Successive generations of smaller amplitudes are seen at "resonance" locations of either

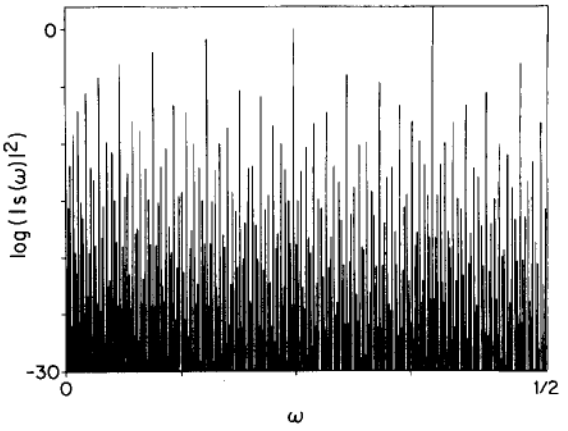

Fig. 1. The ordinary power spectrum for 4181 cycle elements of the standard sine map with $a = 0.98$ and $\rho = 2584/4181$ on a log plot. The principal peaks are located at either $\omega = \langle m\rho \rangle_1$ or $\omega = 1 - \langle m\rho \rangle_1$ for small integers m.

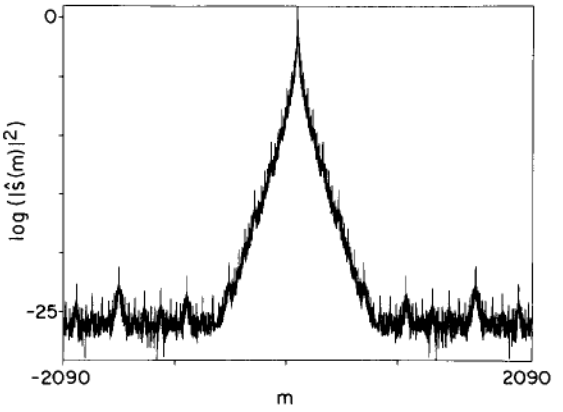

Fig. 2. The reordered power spectrum of fig. 1 with $p/q = 2584/4181$ on a log plot. The single peak at the center decays roughly exponentially. The flat plateau reflects the precision of our computation.

$\omega = \langle m\rho_{17} \rangle_1$ or $1 - \langle m\rho_{17} \rangle_1$, where m is a small integer. A complex structure results since the modular function, $\langle m\sigma \rangle_1$, is not monotonic in m. The relatively sharp peaks and low background noise suggests that the spectrum corresponds to quasiperiodic regime below the chaos transition which is known to occur at $a = 1$.

If we had used a higher order rational approximant to ρ, only the small amplitude peaks of the spectrum would have been significantly affected. The dominant peaks are always determined by low resonances of ρ. These are stable against increasing the order of the rational approximation. The use of successively longer time series data enables us to obtain a systematic and convergent approximation to the Fourier spectrum of the quasiperiodic time series [11].

2.2. *Reordered Fourier spectrum*

2.2.1. *Two-frequency case*

In the previous section, we have demonstrated that $s(\omega)$ is complicated, but hinted at the simplicity of A_n, the Fourier transform of $g(x)$ which contains the dynamical information. We shall now demonstrate the relation between the two. Let us define the "reordered" spectrum $\hat{s}_n(m)$ by

$$\hat{s}_n(m) = s_n\big(\langle mp_n \rangle_{q_n}\big), \tag{2.11}$$

where as before $\langle\ \rangle_{q_n}$ indicates the modulus with respect to q_n. The reordering of fig. 1 is shown in fig. 2, where we have plotted $\log(|\hat{s}_{17}(m)|^2)$ versus m with $p_{17}/q_{17} = 2584/4181$. In contrast to fig. 1, only one major peak is seen in the center. This is the result of the transformation bringing all the low order harmonics of ρ into the neighborhood of the origin. Fig. 2 suggests that the decay of $\hat{s}$ is exponential until it levels off at the limits determined by the accuracy of our computation.

How does the reordered spectrum relate to $g(x)$? By substituting $g(l\rho)$ for x_l and the Fourier series for $g(l\rho)$ into eq. (2.11), we see that

$$\hat{s}_n(m) = \frac{1}{q_n} \sum_{l=0}^{q_n - 1} e^{-2\pi i l m p_n / q_n} \sum_{k=-\infty}^{\infty} A_k e^{2\pi i l k \rho}. \tag{2.12}$$

This can be reduced to

$$\hat{s}_n(m) = \frac{1}{q_n} \sum_{k=-\infty}^{\infty} A_k \frac{1 - e^{2\pi i (k\rho q_n - m p_n)}}{1 - e^{2\pi i (k\rho - m p_n / q_n)}}. \tag{2.13}$$

As $p_n/q_n \to \rho$, the sum is dominated by the term corresponding to $m = k$ and we find

$$\lim_{n\to\infty} \hat{s}_n(m) \to A_m. \tag{2.14}$$

In the irrational limit $q_n \to \infty$, the reordered spectrum is simply equal to the Fourier transform of $g(x)$.

The "quasiperiodic regime" is defined by $g(x)$ being C_∞. Provided a single upper bound exists for all derivatives of $g(x)$, A_m must then decay faster than any power of m for large m [2]. This is certainly the case for the spectrum in figs. 1 and 2.

It is well known that circle map in eq. (2.8) undergoes a transition to chaos at $a = 1$, when the inverse map becomes singular. The function $g(x)$ remains continuous, but is nowhere continuously differentiable. The Fourier amplitudes of $g(x)$ will then decay only as fast as constant/m. This sharp difference between the behavior of the high harmonics can be easily seen in the reordered spectrum and may be used as a guide to determine chaos onset in a more complicated system.

2.2.2. *Three-frequency case*

Let us now assume that $x(t)$ is a dynamical variable of a system with three fundamental frequencies ω_1, ω_2 and ω_3. We can therefore write

$$x(t) = \sum_{n_1, n_2, n_3} a(n_1, n_2, n_3)\, e^{2\pi i \boldsymbol{n}'\cdot\boldsymbol{\omega} t}, \tag{2.15}$$

where $\boldsymbol{n}' = (n_1, n_2, n_3)$ and $\boldsymbol{\omega} = (\omega_1, \omega_2, \omega_3)$. Analogous to the definitions in the previous section, we define the discrete time series $\{x_l\}$ as the values of $x(t)$ obtained by strobing $x(t)$ at discrete time intervals corresponding to a fundamental period, say $2\pi/\omega_3$, so that $x_l = x(2\pi l/\omega_3)$. We define the pair of reduced frequencies to be $\boldsymbol{\rho} = (\rho_1, \rho_2) = (\omega_1/\omega_3, \omega_2/\omega_3)$. According to this definition x_l is given by

$$x_l = \sum_{n_1, n_2} A(n_1, n_2)\, e^{2\pi i l \boldsymbol{n}\cdot\boldsymbol{\rho}}, \tag{2.16}$$

where $\boldsymbol{n} = (n_1, n_2)$, and

$$A(n_1, n_2) = \sum_{n_3 = -\infty}^{\infty} a(n_1, n_2, n_3). \tag{2.17}$$

This is of course a simple extension of the manipulations in the previous section.

If the "fundamental" frequencies ω_1, ω_2 are actually not irrational multiples of each other, and we can find integers p, q and r so that $\boldsymbol{\rho} = (p/r, q/r)$, it is easy to see that $x_l = x_{l+r}$. However, if the fundamental frequencies are irrational multiples of each other, we can still define simultaneous rational approximants $\boldsymbol{\rho}_n = (p_n/r_n, q_n/r_n)$ so that $r_{n+1} > r_n$ and

$$\lim_{n\to\infty} |\boldsymbol{\rho}_n - \boldsymbol{\rho}| = 0$$

and

$$|(p_n, q_n) - r_n\boldsymbol{\rho}| > |(p_{n+1}, q_{n+1}) - r_{n+1}\boldsymbol{\rho}|.$$

For a typical dynamical system, the integers r_n then determine "close returns" of the dynamical system, i.e. there is an integer n'' so that if $n' > n''$, $|x_{l+r_n} - x_l| > |x_{l+r_{n'}} - x_l|$. (Note that this statement is considerably weaker than for the circle map, where $n'' = n$.) Let us assume that we have the time series x_l for a dynamical system with three incommensurate frequencies. We then compute the ordinary discrete Fourier transform, truncating the data to length r_n:

$$s_n(m) = \frac{1}{r_n} \sum_{l=0}^{r_n - 1} x_l\, e^{-2\pi i l m/r_n}, \tag{2.18}$$

where $0 \le m < r_n$. We would now like to relate $s_n(m)$ to $A(\boldsymbol{n})$ as defined in eq. (2.17). This is considerably more complicated than in the two-frequency problem since $s_n(m)$ is determined by a single integer while $A(\boldsymbol{n})$ is determined by an integer pair. But it turns out that we can proceed with a method very similar to that used in the two-frequency problem. We *define* the "reordered"

spectrum as follows:

$$\hat{s}_n(\boldsymbol{m}) = s_n\big(\langle \boldsymbol{m}\cdot\boldsymbol{p}_n\rangle_{r_n}\big), \tag{2.19}$$

where $\boldsymbol{m} = (m_1, m_2)$ and $\boldsymbol{p}_n = (p_n, q_n)$ are integers. Thus, the "reordered" spectrum is a function of two integers, whereas the ordinary Fourier amplitude is determined by a single integer.

It is tempting to let $\boldsymbol{m}$ be all pairs of integers between 0 and r_n. However, these r_n^2 choices are not independent, since there are in fact r_n solutions to $\langle \boldsymbol{m}\cdot\boldsymbol{p}_n\rangle_{r_n} = 0$ in the r_n by r_n square. We can think of $\mathbb{Z}_2$, the space of integer pairs, as defining a "reciprocal" space, with the solutions $\boldsymbol{m}$ of $\langle \boldsymbol{m}\cdot\boldsymbol{p}_n\rangle_{r_n} = 0$ defining a Bravais lattice. This is illustrated in fig. 3, for the case $(p_n, q_n, r_n) = (4, 5, 7)$. The 7×7 lattice of integers in fig. 3 represent the values of $\langle 4m_1 + 5m_2\rangle_7$ for $0 \le m_1, m_2 < 7$. Basis vectors of the Bravais lattice for this example are chosen to be $\boldsymbol{b}_0 = (4, 1)$ and $\boldsymbol{b}_1 = (1, 2)$ which are represented by arrows in fig. 3. The "fundamental domain" of the Bravais lattice is determined by the parallelopiped defined by these basis vectors. There is a 1 : 1 correspondence between each element in the fundamental domain and each independent spectral amplitude. Note that the vectors obey $|\boldsymbol{b}_0 \times \boldsymbol{b}_1| = 7 = r_n$ as they must in order for the fundamental domain determined by the Bravais lattice to define the correct number of independent amplitudes. Thus, the reordered spectrum is naturally viewed as a function of two integers in the fundamental domain.

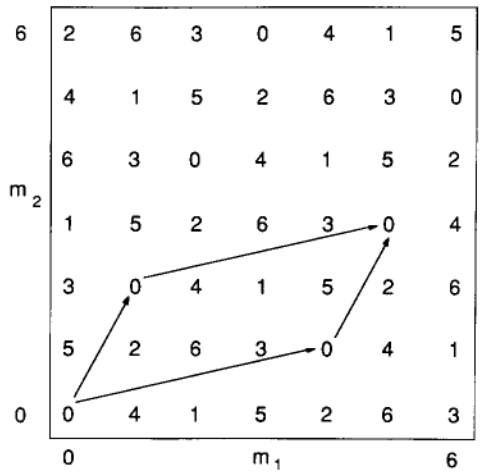

Fig. 3. The reciprocal lattice for $(p, q, r) = (4, 5, 7)$ is shown. The 7×7 lattice of integers represents the value of $\langle 4m_1 + 5m_2\rangle_7$ for $0 \le m_1, m_2 < 7$. Two arrows represent the basis vectors of the reciprocal lattice.

What can we learn by looking at $\hat{s}_n(\boldsymbol{m})$ rather than $s_n(m)$? From eq. (2.16), we define the function

$$g(\theta_1, \theta_2) = \sum_{n_1, n_2} A(n_1, n_2)\, e^{2\pi i(n_1\theta_1 + n_2\theta_2)}. \tag{2.20}$$

According to this definition, $x_l = g(\langle l\rho\rangle_1)$ where $\langle (x_1, x_2)\rangle_1 = (\langle x_1\rangle_1, \langle x_2\rangle_1)$. Thus, again we say that $g(\theta_1, \theta_2)$ generates the dynamics of x_l. We know from previous work, both from conventional rigorous methods [8] and from RG methods [4] that for at least a mapping with sufficiently weak nonlinearity, $g(\theta_1, \theta_2)$ will be a C_∞ function of θ_1 and θ_2. Therefore, we expect $A(n_1, n_2)$ to decay with an increasing modulus in $\boldsymbol{n} = (n_1, n_2)$ sufficiently rapidly to allow all derivatives of $g(\theta_1, \theta_2)$ to exist. These arguments show that $A(\boldsymbol{n})$ will be a function strongly peaked near the origin and decaying faster than any power law with increasing radius in $\boldsymbol{n}$. As for the 2-frequency problem, $A(\boldsymbol{n})$ is essentially the reordered spectrum. We shall now relate $A(\boldsymbol{n})$ to $\hat{s}_n(\boldsymbol{m})$.

By the definition of g

$$A(\boldsymbol{m}) = \int_{\boldsymbol{\theta}} e^{-2\pi i \boldsymbol{m}\cdot\boldsymbol{\theta}} g(\boldsymbol{\theta})\, d^2\theta, \tag{2.21}$$

where $\boldsymbol{\theta} = (\theta_1, \theta_2)$. Since $\langle l\rho\rangle_1$ covers the unit square uniformly,

$$\begin{aligned} A(\boldsymbol{m}) &\sim \frac{1}{r_n}\sum_{l=0}^{r_n-1} e^{-2\pi i l\rho_n\cdot\boldsymbol{m}} g(\langle l\rho_n\rangle_1) \\ &= \frac{1}{r_n}\sum_{l=0}^{r_n-1} x_l\, e^{-2\pi i lk/r_n}, \end{aligned} \tag{2.22}$$

where $k = \langle \boldsymbol{m}\cdot(p_n, q_n)\rangle_{r_n}$. Hence

$$A(\boldsymbol{m}) = \lim_{n\to\infty} \hat{s}_n(\boldsymbol{m}). \tag{2.23}$$

This shows that the "reordered" spectrum should be strongly peaked near the origin, and decay quickly as a function of $|m|$.

3. Numerical analysis of the reordered Fourier spectrum

3.1. *Circle maps*

As a numerical example, we study the "standard" sine map introduced in section 2.2.1:

$$x_{n+1} = f_{a,\Omega}(x_n) = x_n + \Omega - \frac{a}{2\pi}\sin(2\pi x_n), \quad (3.1)$$

using the golden mean winding number, $\rho = \sigma_G = (\sqrt{5}-1)/2$. The critical value of "a" when dynamics changes from quasiperiodic to chaotic is known to be 1. The ordinary power spectrum of 4181 cycle elements of the critical sine map ($a = 1$) with $\rho = 2584/4181$ is shown in fig. 4. Except for the overall rise of the noise, it is difficult to see a qualitative change of the spectrum from the subcritical case ($a = 0.98$) in fig. 1.

The reordered power spectrum on a log plot is obtained by plotting m versus $\log(|\hat{s}(m)|^2)$, where $\hat{s}(m) = s(\langle 2584m\rangle_{4181})$ is shown in fig. 5. Note the dramatic difference between the critical reordered power spectrum and the subcritical one shown in fig. 2. For the subcritical spectrum, the peak around the center of the reordered power spectrum decays roughly exponentially in m. At criticality, the central peak decays algebraically in m. In order to determine the critical behavior, the reordered power spectrum is rescaled by m. The plot of m versus $\log(m^2|\hat{s}(m)|^2)$ in fig. 6 suggests that $|\hat{s}(m)| \approx 1/m$. The sharp crossover between two spectra could, in principle, be used to determine the critical value of a nonlinear parameter of the given dynamical system.

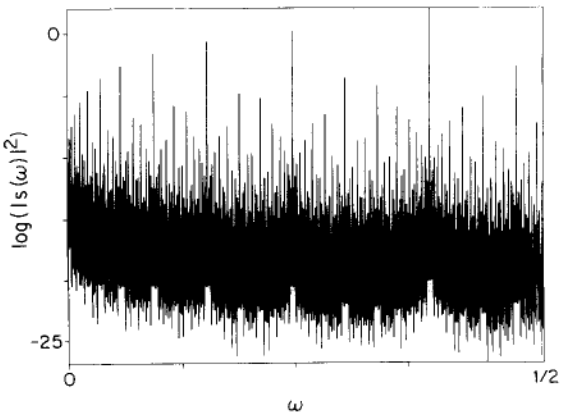

Fig. 4. Similarly to fig. 1, the ordinary power spectrum of the critical sine map at $a = 1$ is shown.

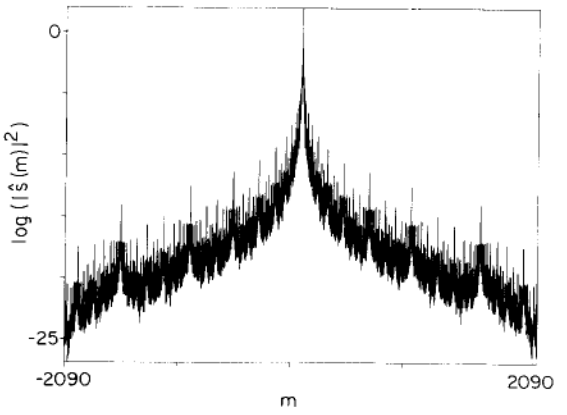

Fig. 5. The reordered power spectrum of fig. 4 on a log plot as in fig. 2. Note that the overall background noise has risen. This noise comes from the approach to chaos in the dynamics, *not* from computational error.

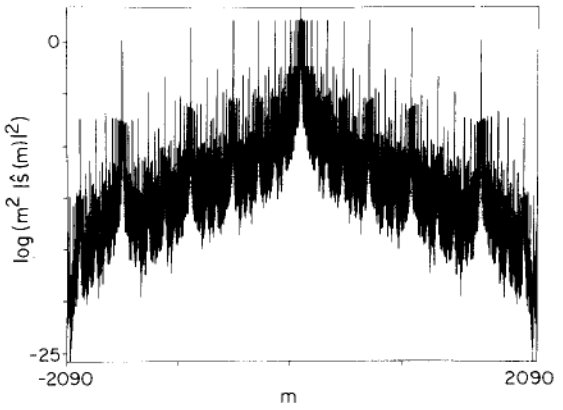

Fig. 6. The power spectrum of fig. 5 after being multiplied by m^2 is shown. Note that almost all the major peaks are of comparable heights, which suggests $\hat{s}(m) \approx 1/m$.

3.2. *Torus maps*

For three-frequency systems, "strongly coupled" torus maps are used for our numerical analysis:

$$\begin{pmatrix} x_{n+1} \\ y_{n+1} \end{pmatrix} = \boldsymbol{F}_{a,\boldsymbol{\Omega}}(x_n, y_n)$$

$$= \begin{pmatrix} x_n + \Omega_x - \dfrac{a}{2\pi}\sin(2\pi y_n) \\ y_n + \Omega_y - \dfrac{a}{2\pi}\sin(2\pi x_n) \end{pmatrix}, \qquad (3.2)$$

where $\boldsymbol{\Omega} = (\Omega_x, \Omega_y)$ is a vector of fixed parameters which determines the rotation rate, $\boldsymbol{\rho}$, and "a" controls the nonlinearity of the system. We will choose $\boldsymbol{\rho}$ to be the "spiral mean", $\boldsymbol{\rho}_S = (1/\tau^2, 1/\tau)$, where τ satisfies $\tau^3 = \tau + 1$, $\tau = 1.3268\ldots$. For this choice of $\boldsymbol{\rho}$, the critical value of "a" above which the Jacobian of the highly iterated map becomes singular is known to be $a_c = 0.882 \pm 0.003$ [4].

The ordinary power spectrum for 5842 cycle elements of a subcritical torus map with $\boldsymbol{\rho} = (3329/5842, 4410/5842)$ is shown in fig. 7 for $a = 0.7$. The time series used for the Fourier transform is chosen to be the modulus of $\boldsymbol{x}_l$, where $\boldsymbol{x}_l = \boldsymbol{f}^l(\boldsymbol{x}_0) - l\boldsymbol{\rho} - \boldsymbol{x}_0$. $\boldsymbol{x}_0$ is a member of maximally stable 5841 cycles. Two major peaks are seen at $\omega_1 = 1513/5842$ and $\omega_2 = 1432/5842$. The corresponding peaks for $\omega > \frac{1}{2}$ are at $\omega_1' = 3329/5842$ and $\omega_2' = 4410/5842$.

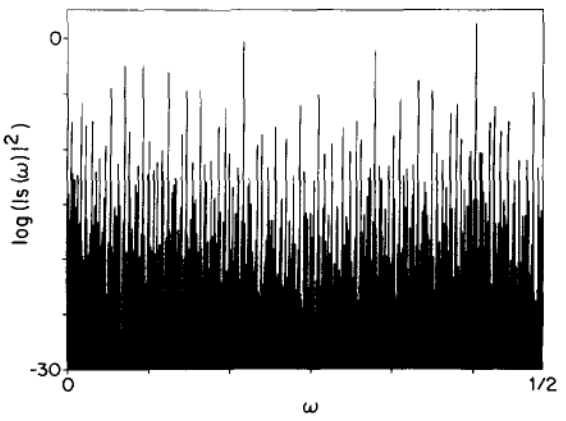

Fig. 7. The ordinary (subcritical) power spectrum for 5842 cycle elements of a strongly coupled torus map with $a = 0.7$ and $\boldsymbol{\rho} = (3329/5842, 4410/5842)$ on a log plot.

The fundamental domain of the reordered spectrum in the reciprocal lattice is defined by two basis vectors $\boldsymbol{b}_1 = (-56, 33)$ and $\boldsymbol{b}_2 = (26, 89)$. Two vectors reciprocal to the reciprocal lattice are given by $\boldsymbol{k}_1 = (89, -33)/5842$ and $\boldsymbol{k}_2 = (-26, 56)/5842$. In order to better determine the change of the spectrum near the criticality, the reordered power spectrum is rescaled by a factor $r_s(\boldsymbol{m})$ which measures a distance from an origin to $\boldsymbol{m}$. Our choice is $r_s(\boldsymbol{m}) = (\alpha_1(\boldsymbol{m})^2 + \alpha_2(\boldsymbol{m})^2)^{1/2}$, where $\alpha_i(\boldsymbol{m}) = \boldsymbol{k}_i \cdot \boldsymbol{m} - [\boldsymbol{k}_i \cdot \boldsymbol{m}]$ for $i = 1, 2$. $[x]$ denotes the largest integer less than or equal to x. If $\alpha_i(\boldsymbol{m}) > \frac{1}{2}$ then $\alpha_i(\boldsymbol{m}) = 1 - \alpha_i(\boldsymbol{m})$. The function r_s is chosen to satisfy the periodic boundary conditions on the Brillouin zone boundaries. Fig. 8 shows the plot of $\boldsymbol{m}$ versus $(r_s(\boldsymbol{m})|\hat{s}(\boldsymbol{m})|)^2$, where $\hat{s}(\boldsymbol{m}) = s(\langle \boldsymbol{m} \cdot (3329, 4410)\rangle_{5842})$. Instead of the Brillouin zone, the region around the origin roughly equivalent to the area of the first Brillouin zone is chosen to be the domain of $\boldsymbol{m}$ due to limitation of the graphic software available to us. The existence of a peak structure around the origin decaying rapidly in $|\boldsymbol{m}|$ suggests that the map is subcritical. The reordered power spectra corresponding to higher values of a, $a = 0.85$ and $a = a_c \approx 0.882$, are shown in fig. 9 and fig. 10, respectively. Note that small peaks near the left corners of the figs. 9

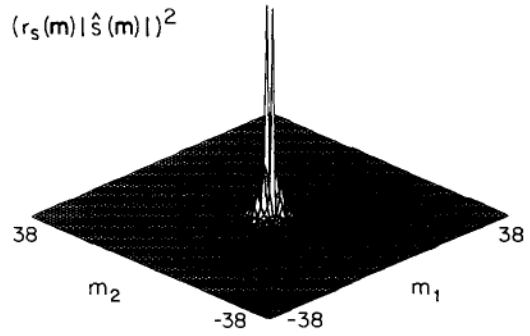

Fig. 8. The reordered power spectrum of fig. 7 with $(p/r, q/r) = (3329/5842, 4410/5842)$ is shown after rescaling by r_s. The function r_s is roughly proportional to the distance of a Fourier peak from the origin. The domain of $\boldsymbol{m}$ is roughly the size of the first Brillouin zone. Actual values of peaks are not shown since we are interested only in the relative strength of peaks.

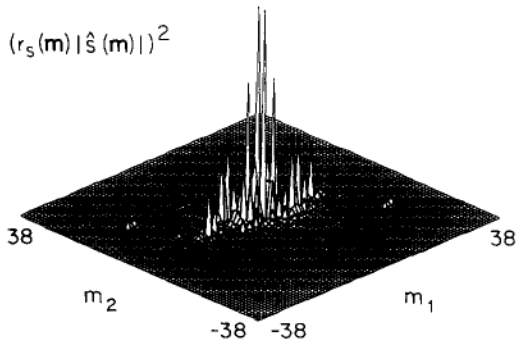

Fig. 9. The reordered power spectrum for $a = 0.85$ as in fig 8. Note the appearance of small peaks around the left corner due to noise in time series.

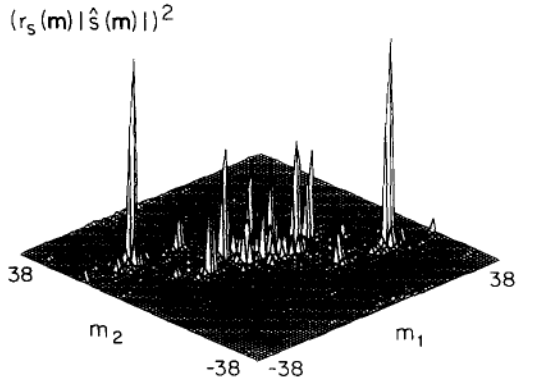

Fig. 10. The critical reordered power spectrum for $a = a_c \approx 0.882$ as in fig. 8.

and 10 grow rapidly as "a" increases. At criticality shown in fig. 10, these peaks become comparable to the main peaks around the center suggesting $|\hat{s}(\boldsymbol{m})| \approx 1/|\boldsymbol{m}|$, and that the function $g(x)$ is not continuously differentiable.

3.3. *Experimental time series*

Although we do not intend to present an exhaustive analysis of the time series of experimental systems, we would like to demonstrate that the reordering scheme also works for experimental data with noise and other non-ideal factors.

We study as an example a time series obtained from the Rayleigh–Bénard convection experiment of Gollub and Benson [6]. Though there are many qualitatively different types of time dependent states of a convective flow depending on experimental configurations, we investigate only one quasiperiodic state with two incommensurate frequencies [12] whose configuration corresponds to fig. 8(b) of ref. [6]. We refer the readers to ref. [6] for details on the experiment.

Here the time series represent the local velocity of a convecting fluid in a box measured at evenly spaced time intervals. The ordinary power spectrum of time series of this quasiperiodic state is shown in fig. 11. All peaks are integral combinations of two fundamental peaks at $\omega_1 = 0.04624$ and $\omega_2 = 0.12582$. The subjective error bar for the values of ω is 5×10^{-6}. There are two major peaks for $\omega > \frac{1}{2}$ corresponding to the reflection about $\omega = \frac{1}{2}$ of peaks at ω_1 and ω_2. The values of ω for these mirror peaks are used to form a 2-d winding vector, $\boldsymbol{\rho} = (0.95376, 0.87418)$. The simultaneous rational approximation to $\boldsymbol{\rho}$ can be conveniently done by the generalized Farey tree algorithm [13]. The 33rd simultaneous Farey rational approximant, $(p/r, q/r) = (743/779, 681/779)$, is used to generate the reordered spectrum.

The fundamental domain is defined by two basis vectors $\boldsymbol{b}_1 = (-3, 17)$ and $b_2 = (43, 16)$. Two vectors reciprocal to the reciprocal lattice are $\boldsymbol{k}_1 = (16, -17)/779$ and $\boldsymbol{k}_2 = (-43, -3)/779$. The re-

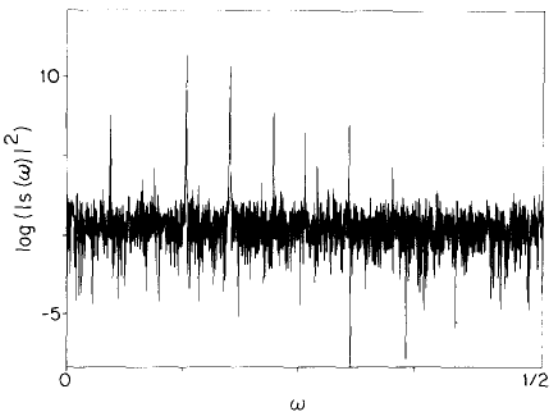

Fig. 11. The ordinary power spectrum of a time series from the convection experiment of Gollub and Benson. Two major peaks are seen at $\omega = 0.04624$ and $\omega = 0.12582$.

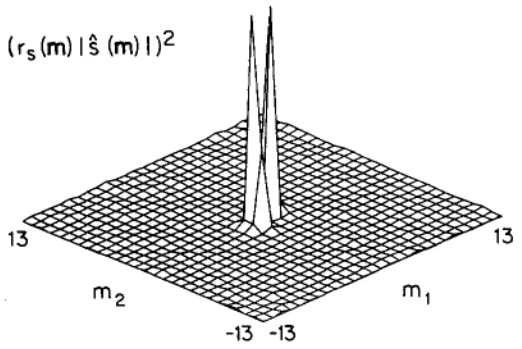

Fig. 12. The reordered power spectrum of fig. 11 with $(p/r, q/r) = (743/779, 681/779)$ after rescaling by r_s.

scaling function r_s of Fourier amplitudes is the same as one used in the previous section. Fig. 12 shows the plot of $\boldsymbol{m}$ versus $(r_s(m)|\hat{s}(\boldsymbol{m})|)^2$, where $\hat{s}(\boldsymbol{m}) = s(\langle \boldsymbol{m} \cdot (743, 681)\rangle_{779})$. As before the region around the origin roughly equivalent to the area of the first Brillouin zone is chosen to be the domain of $\boldsymbol{m}$. The existence of the single peak at the center confirms that there are only two independent modes in the experimental system. The decay of a peak at the center even after rescaling suggests that the system is subcritical. The small ripples away from the center is the indication of the existence of a small noise in the experimental time series.

4. Discussions and conclusions

Though there is virtually no limit to the accuracy with which we can analyze the reordered spectra for cycle elements of *maps*, the analysis of the experimental time series involves several complications.

First, the fundamental frequencies of the experimental time series cannot be determined with the arbitrary precision. For example, the drift of the fundamental frequencies can cause an uncertainty in determining the fundamental frequencies, broadening the fundamental peaks in the Fourier spectrum. If the denominator of a rational approximant to a set of fundamental frequencies chosen for reordering is too large, peaks on the shoulders of the major peaks may be mapped away from the origin by the reordering transformation. Therefore relatively strong peaks should appear away from the origin in the reordered spectrum. Choosing the rational approximant with a sufficiently small denominator can reduce these side peaks. On the other hand, the denominator of the rational approximant cannot be too small in order for the resulting reordered spectrum to contain enough sharp harmonics to determine the decay property of the central peak structure. Our example of the experimental time series in section 3.3 shows that the drift is small enough to enable us to pick a rational approximant satisfying the above criteria.

Though less serious it may appear, the finiteness of the experimental time series also may hinder the reordering analysis. If the number of time series used for the Fourier spectrum is N the naive estimate of the maximal uncertainty for the fundamental frequencies is $1/N$. It is known, however, that the fundamental frequencies can be more accurately determined by interpolating several Fourier amplitudes around the major peak to obtain the frequency corresponding to the maximum amplitude. Since the discontinuity of time series at the ends of sampling interval usually leads to the less accurate amplitudes for the Fourier peaks, it is necessary to modulate the time series by a smooth function, called a window function, vanishing at the initial and final times to obtain the spectrum closer to the true spectrum [14]. The accuracy of a few parts in a million can be achieved by this method when time series with roughly 2000 data points is used, which appears to be sufficient to separate quasiperiodic dynamics from chaotic one.

Another complication for the experimental time series is the presence of external noise. If time series contain random noise, the ordinary spectrum will exhibit the background noisy peaks with uniform strength. The reordered spectrum rescaled by $|\hat{s}(m)|^2 \to |m|^2|\hat{s}(m)|^2$ will show the background noisy peaks whose envelope grows quadratically in $|m|$. However, the reordered spec-

trum for the time series at the chaos onset, if rescaled, should show almost uniformly strong peaks regardless of the distance from the origin. Therefore, as long as the noise is reasonably small, the noise peaks will be relatively small near the origin and will not interfere with the observation of the central peak structure near origin in determining the chaos onset. The numerical study suggests that the incorporation of the random noise does not destroy the main feature of the reordered spectrum even when the strength of noise is about 10 percent of the signal amplitude.

How well does our reordering analysis work in determining the critical parameter values for the chaos transition? We do not necessarily expect that the reordering spectral analysis would work better than the numerical determination of the criticality as discussed in ref. [13]. The latter is computationally easier for time series from mappings. For experimental time series, however, the reordered spectral analysis may determine the criticality better than the ordinary Fourier analysis since the former enables us to separate the noise effect from the true dynamics of time series at the chaos onset. Moreover, the observation of the growth of a single peak or a couple of peaks in the reordered spectrum is easier and more controllable than the conventional method of the minimization of the sum of differences of the actual peak positions and fitted ones from the low order combinations of fundamental frequencies [6]. Without an extensive analysis of the experimental data, however, our answer is qualitative at best.

We have shown how to reorder spectral data from the time series to give information about quasiperiodic and chaotic behavior of the underlying dynamics. Though only two or three frequency systems are studied in this paper, the reordering scheme can be also applied to systems with more than three fundamental frequencies, provided we use sensible simultaneous rational approximation schemes. It is our hope that future investigations will find this method particularly useful in probing the properties of the multi-frequency dynamical systems, and we believe that it can be a useful experimental tool as well as theoretical one.

Acknowledgements

We would like to thank Jerry Gollub and Tom Solomon for communicating their experimental results. This research was supported by the NSF under contract DMR-8519059 at the Laboratory for the Research in the Structure of Matter at the University of Pennsylvania and by NSF contract DMR-8414640.

References

[1] M.J. Feigenbaum, L.P. Kadanoff and S.J. Shenker, Physica 5D (1982) 370.
[2] S. Ostlund, D. Rand, J. Sethna and E. Siggia, Physica 8D (1983) 303.
[3] C. Grebogi, E. Ott and J. Yorke, Physica 15D (1985) 354.
[4] S. Kim and S. Ostlund, Phys. Rev. Lett. 55 (1985) 1165.
[5] G.A. Held and C. Jeffries, Phys. Rev. Lett. 56 (1986) 1183.
[6] J.P. Gollub and S.V. Benson, J. Fluid Mech. 100 (1980) 449.
[7] J. Stavans, F. Heslot and A. Libchaber, Phys. Rev. Lett. 55 (1985) 596.
[8] M.R. Herman, Publications of Paris I.H.E.S. 49 (1979) 1.
[9] P. Cvitanovic, B. Shraiman and B. Soderberg, Phys. Scripta 32 (1985) 263.
[10] S. Ostlund and S. Kim, Renormalization of quasiperiodic mappings, Phys. Scripta T9 (1985) 193.
[11] Convergence here is used in a loose sense; it is only the convolution of the spectrum with a narrow weight function which converges.
[12] This quasiperiodic state actually has only two intrinsic frequencies. Since the strobing time interval used in acquiring time series data is chosen arbitrarily, an additional frequency scale is induced to the time series, making the system be effectively one with three frequencies.
[13] S. Kim and S. Ostlund, Phys. Rev. A 34 (1986) 3426.
[14] C.C. Martens and G.S. Ezra, J. Chem. Phys. 83 (1985) 2990.